

DISK LOADED WAVEGUIDE PARAMETERS FOR ACCELERATION OF PARTICLES WITH INTERMEDIATE MASS IN THE MEDIUM ENERGY RANGE

V.V. Paramonov

*National Research Nuclear University “Moscow Engineering Physics Institute”, Moscow, Russia
E-mail: paramono@inr.ru*

The Disk Loaded Waveguide (DLW) parameters are considered for the L-band frequency range and particle velocity $0.04 < \beta < 1$. Basing on particularities of acceleration with traveling wave, deep optimization of DLW cells dimensions, the choice of optimal operating phase advance for each DLW section and combination of forward and backward wave modes, it is possible to create an effective acceleration system for muons acceleration in the velocity range $0.2 < \beta < 1$, in some parameters overcoming accelerating system with RF cavities in standing wave mode.

PACS: 29.20.Ej

INTRODUCTION

In particle accelerators the DLW structure is now mostly distributed and investigated accelerating structure for acceleration of lightweight particles – electrons in the high energy range, $\beta \sim 1$. Naturally realizing advantages of the Traveling Wave (TW) mode, short pulse operation at the S-band and higher frequencies, DLW is now dominating normal conducting accelerating structure for these applications. In the L-band frequency range also there are proposals and examples of DLW applications for e^- or e^+ acceleration [1, 2]. For lower, than L-band, frequencies DLW is not effective and there are no examples of applications.

For electrons acceleration the DLW period length d_p is constant and matched for particles velocity $\beta=1$. Acceleration of hadrons in medium β range for linear accelerators naturally leads to the requirements of lower frequencies and Standing Wave (SW) operation with longer RF pulse. The length of period for accelerating structure for hadrons is variable and follows to the growing velocity of particles.

Comparing the rest energies for protons W_{rp} , muons W_{rm} and electrons W_{re} , we have $W_{rp}=938.28$ MeV, $W_{rm}=105.66$ MeV and $W_{re}=0.511$ MeV, respectively. From this comparison acceleration of muons looks more similar to acceleration of protons. Nevertheless, muons are one order lighter than protons, and it looks useful to consider solutions, developed for electrons acceleration with DLW, for muons acceleration.

The goal of this work is to consider possibility of the DLW structure application for muons acceleration in medium and low, as possible, energy range.

1. DLW PARAMETERS STUDY

The distribution of the longitudinal electric field in the aperture of the DLW in TW operating mode can be presented as the sum over spatial harmonics, see, for example [3].

$$E_z(r, z) = \sum_{-\infty}^{\infty} E_n I_0(k_{rn} r) e^{-ik_{zn} z}, \quad E_n = \frac{1}{d_p} \int_0^{d_p} E_z(r, z) e^{ik_{zn} z}, \quad (1)$$

$$k_{zn} = \frac{\theta + 2n\pi}{d_p}, \quad n = 0, \pm 1, \dots, \pm \infty, \quad k_{rn}^2 = k_{zn}^2 - k^2, \quad k = \frac{2\pi}{\lambda},$$

where E_n is the amplitude of the n -th spatial harmonic, $I_0(k_{rn} r)$ is the modified Bessel function, λ is the operating wavelength and θ is the operating phase advance. Usually the fundamental, main, spatial harmonic $n=0$ is

used for acceleration, due to large E_0 value. This case DLW has a positive dispersion and operates in Forward Wave (FW) TW mode.

Acceleration with the first nearest spatial harmonic $n = -1$ is also possible [3], there are a lot of papers with proposals, but for $\beta \sim 1$ loses in RF efficiency, because $|E_0| > |E_{-1}|$. Until now just one practical application using DLW with the first harmonic $n = -1$ is known with an interesting result for particles focusing [4, 5]. Such case DLW operates in Backward Wave (BW) TW mode and has the negative dispersion, β_g .

Parameters of the DLW structure were calculated and stored in a data library in the same procedure, as described in [6] both for fundamental $n=1$ and the first $n = -1$ harmonics, assuming operating frequency 1296 MHz. The considered shape of DLW cells is shown in Fig. 1 for different β and θ combinations.

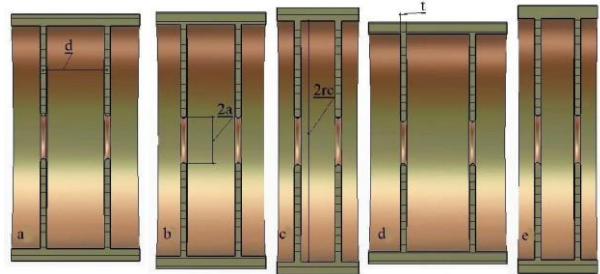


Fig. 1. The DLW geometry for FW operation $\beta=0.90$, $\theta=90^\circ$ (a); $\beta=0.57$, $\theta=120^\circ$ (b); $\beta=0.41$, $\theta=120^\circ$ (c); BW operation $\beta=0.41$, $\theta=120^\circ$ (d); $\beta=0.20$, $\theta=120^\circ$ (e)

The length of the cell – the period length d_p is defined for FW or BW operation as

$$d_p = \frac{\beta\lambda\theta}{2\pi}, \quad n = 0, \quad d_p = \frac{\beta\lambda(2\pi - \theta)}{2\pi}, \quad n = -1. \quad (2)$$

More complicated shape, similar to [2], also can be considered if more deep optimization will be required. More details about DLW parameters study one can find in [7].

The main parameter for DLW TW operation is the group velocity value β_g . The surfaces $\beta_g(a/\lambda, \theta)$ are shown in the Fig. 2 for different β values both for FW (the top row in Fig. 2) and BW operation (the bottom row in Fig. 2). Both for FW and BW operation for the constant aperture radius $a = const$ one can see sin-like dependence β_g on θ for all β values. For the fixed phase advance θ there is a fast rise $\beta_g \sim a^3$ with aperture increasing.

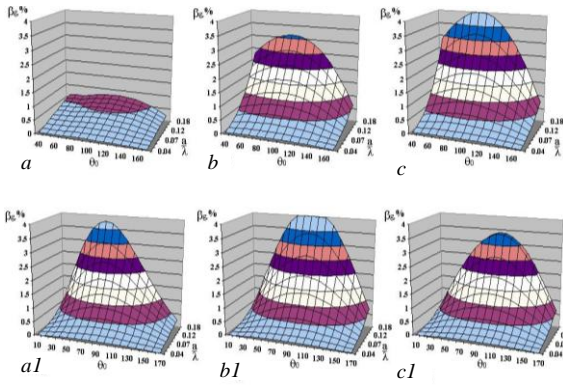


Fig. 2. The surfaces $\beta_g(a/\lambda, \theta)$ for $\beta=0.22$ (a, a1), $\beta=0.57$ (b, b1) and $\beta=0.92$ (c, c1). The top line - FW $n=0$ operation, the bottom line - BW $n=-1$ operation, $t=5$ mm

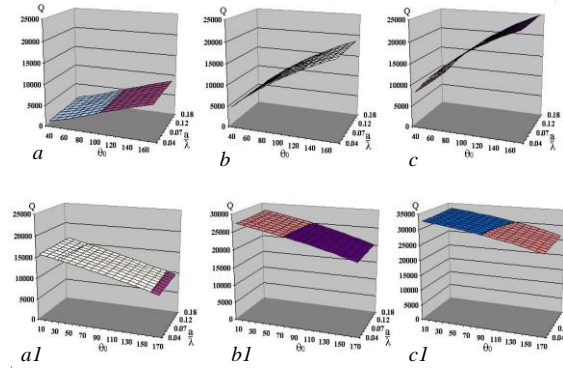


Fig. 3. The surfaces $Q(a/\lambda, \theta)$ for $\beta=0.22$ (a, a1), $\beta=0.57$ (b, b1) and $\beta=0.92$ (c, c1). The top line - FW $n=0$ operation, the bottom line - BW $n=-1$ operation, $t=5$ mm

Another important parameter of DLW cells is the quality factor Q and the surfaces $Q(a/\lambda, \theta)$ are shown in Fig. 3 for different β values both for FW (the top row in Fig. 3) and BW operation (the bottom row in Fig. 3). The structure operates in TM_{01} -like mode and the main parameter, which defines Q value, is the ratio of the cell length to the cell radius. As one can see from the surfaces in Fig. 3, there are no essential Q dependence on the aperture radius a . For lower β values quality factor decreases, especially for FW operation. With θ decreasing d_p decreases for FW operation and increases for BW one, (2). It explains the opposite slope of surfaces in Fig. 3 for FW and BW waves. For the first synchronous harmonic $n=-1$ the cell length d_p is all time larger, than for synchronous fundamental harmonic $n=0$ and quality factor is higher all time. It results in lower wave attenuation for BW operation.

1.1. MAIN RELATIONS AND SCALING

Another RF parameters of the structure are connected with relations:

$$\alpha = \frac{\pi}{\lambda \beta_g \cdot Q} \cdot \frac{E_n}{\sqrt{P_t}} = \sqrt{\frac{2\pi Z_{en}}{\beta_g \lambda Q}}, Z_{en} = \frac{\left| \int_0^{d_p} E_z(0, z) \cdot e^{ik_n z} dz \right|^2}{P_s \cdot d_p}, \quad (3)$$

where α , Np/m is the attenuation constant per unit length, λ – is the operating wavelength, P_t and P_s are the RF power flux and the RF losses in the surface, E_n , MV/m and Z_{en} , MOhm/m are the accelerating gradient and effective shunt impedance for the n -th synchronous harmonic, respectively.

For the main harmonic $n=0$, using some assumptions for the field distribution in the DLW cell, the field decay in the DLW aperture, Fig. 4,a, one can get [7] a simplified estimation for E_0 , which provides $\sim 20\%$ overestimation in E_0 value, but shows very well $E_0(\beta)$ relation, see [7] for explanations.

$$\frac{E_0}{\sqrt{P_t}} \approx 100 \cdot \frac{F(a, \beta, \lambda)}{\lambda \sqrt{\beta_g}}, \quad (4)$$

$$F(a, \beta, \lambda) = I_0 \left(\frac{2\pi a}{\beta \lambda} \sqrt{1 - \beta^2} \right),$$

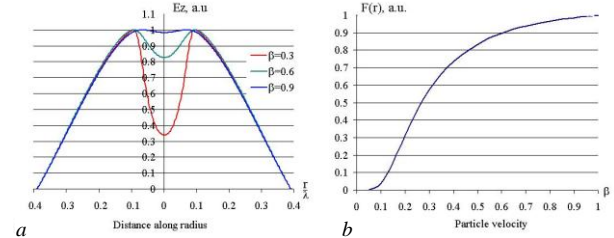


Fig. 4. E_z distribution along radius for different β values at the distance $d_p/3$ from the iris center (a) and the plot of the function $F(a, \beta, \lambda)$ for $a/\lambda=0.08$, (b)

The plot of the function $F(a, \beta, \lambda)$, (4), is shown in Fig. 4,b. This function reflect the natural effect of the decay for harmonics from the aperture radius a to the beam axis. This effect is common for all accelerating structures, but for DLW it is sharpened by relatively large a value, required to obtain the required β_g value. It is one of the restricting factors for DLW application in FW mode at low particles velocity.

From (3) and (4) one can see, that scaling with frequency is $\alpha \sim f^{3/2}$ for attenuation constant and $E_0 \sim f$ for accelerating gradient.

For the relatively low frequency in the L-band range, as compared to the S-band and higher frequencies, to get significant value of accelerating gradient with necessity we should provide the higher RF power flux P_t (providing higher input RF power P_{in} and select β_g value as small, as possible. It explains relatively low $\beta_g < 0.6\%$ values, suggested in [1, 2]. But β_g defines the sensitivity of DLW RF parameters to the errors and deviations in cell frequencies δf_c during construction. All time the additional procedure – RF tuning of the brazed DLW sections is required in construction. There are modern methods for this procedure, see for example [8], but, anyhow, this procedure takes efforts and increases costs. To compare different options of DLW sections, at least approximately, we introduce a parameters T_c – tuning costs, or tuning efforts, basing on relations:

$$\frac{\delta \theta}{\theta} = \frac{\delta f_c}{\beta_g f_c}, T_c = \sum_1^N \frac{1}{\beta_g}, \quad (5)$$

where N is the total number of DLW cells in the section. This parameters is based on general idea – tuning efforts for the section are the more than larger is number of cells in the section and than β_g is smaller.

1.2. PARAMETERS OPTIMIZATION

For DLW application in the L-band range the reduced iris thickness t , see Fig. 1, is preferable to get the maximal E_0 and the energy gain δW with DLW section. In Fig. 5,a are shown the plots of the maximal E_0 values

assuming $P_t=1$ MW, $\beta_g=0.01$ for different iris thickness t and with the optimal θ value [7]. Corresponding plots of E_{smax}/E_0 ratio are shown in Fig. 5,b.

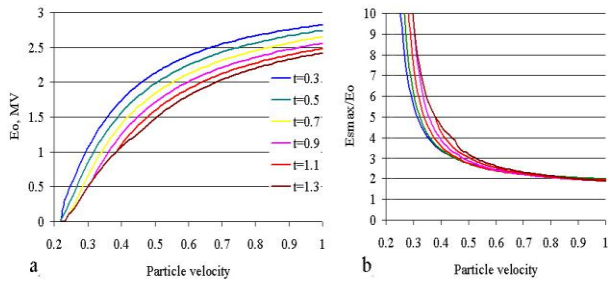


Fig. 5. The plots of the maximal E_0 values for $P_t=1$ MW, $\beta_g=0.01$ (a) and plots of E_{smax}/E_0 ratio (b)

As one can see from Fig. 5,a, for thin iris we can obtain higher E_0 value even with E_{smax} decreasing, Fig. 5,b. With the thinner iris we obtain the required β_g value with smaller aperture radius a . It results in E_0 increasing and already compensates partially E_{smax} increasing due to smaller t . For medium and low β values the effect of field decay, (5) emphasizes E_{smax} decreasing even for small a reduction (see Fig. 5,b). Also with t reduction slightly increases the Q factor of the cell and decreases attenuation α . Totally it leads to the higher δW for DLW section. The iris thickness should be as minimal, as possible, from mechanical rigidity and heat transfer requirements. In the DLW operations with a short RF pulse the average heat loading is negligible and heat transfer limitations are not required.

The muons are not stable particles and should be accelerated as fast as possible, with the maximal possible E_0 value. For FW DLW sections the constant gradient option is reasonable. This case each section has the input and output values of group velocity, β_{gin} , β_{gou} . In Fig.6a with dotted lines are shown plots $E_0(\theta)$ for input particle velocity $\beta_{in}=0.56$ (blue), $\beta_{in}=0.79$ (green) and $\beta_{in}=0.89$ (red curves), for $\beta_g=0.6\%$, $P_t=18$ MW, according (3). One can see E_0 maximum (12~15) MV/m at low θ , near $\theta \sim 90^\circ$ for $\beta_{in}=0.5$, moving to $\theta \sim 75^\circ$ for $\beta_{in}=0.89$. With solid lines in Fig. 6,a are shown plots $E_0(\theta)$, realized in DLW sections with the length $L \sim 2.5$ m, ~ 3.17 m, ~ 3.3 m for the same β_{in} and P_t values, assuming $\beta_{gou}=0.6\%$. The maximal E_0 values shift to higher θ , from $\theta \sim 90^\circ$ to $\theta \sim 120^\circ$. If we select low $\theta \sim 75^\circ$, (see [7] for more explanations), we have in the section beginning, near RF input, shorter cells with lower Q and higher attenuation α . To compensate larger wave attenuation, we have to change β_g value along the section faster. Assuming the same β_{gou} value, it results in larger β_{gin} for low θ and related E_0 reduction, (3). The plot of the difference $\beta_{gin} - \beta_{gou}$ is shown in Fig. 6,b.

To the section end with lower β_g the wave comes already more attenuated and better DLW performance for higher β (see Fig. 4,b; Fig. 7,a and (4)) are less realized. The shift between maximal E_0 values on dotted and solid lines in Fig. 6,a depends on the total attenuation τ in the section.

The maximum of realized E_0 is smooth enough and the relative difference in δW is not more than 3% between $\theta \sim 90^\circ$ and $\theta \sim 120^\circ$ for $\tau \sim 0.25$ Np. But there is essential difference in the number of cells in the section N , Fig. 6,c, leading to significant T_c , (5), reduction,

Fig. 6,d. Additionally, for higher θ the distance between adjacent irises is larger. Selecting θ value for DLW sections, we have to take into account such practical points also.

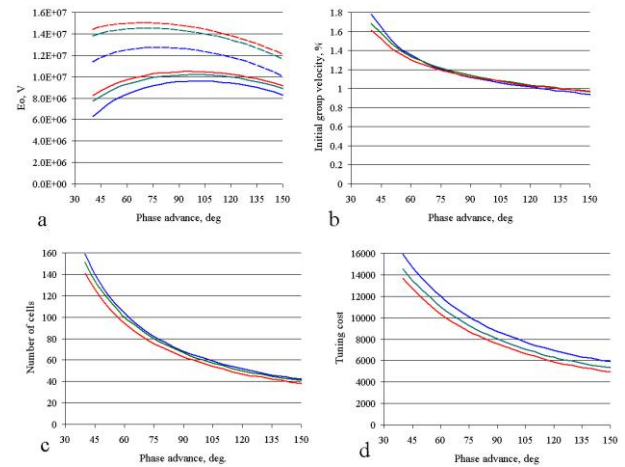


Fig. 6. For constant gradient DLW sections (see text), the maximal possible E_0 (dotted curves) and realized E_0 (solid curves) values, (a), the initial group velocity β_{gin} assuming $\beta_{gou}=0.6\%$ (b), the number of cells in the DLW sections (c) and the 'tuning costs' for sections (d)

2. FORWARD AND BACKWARD WAVE OPERATION

The comparison of the maximal E_n values, (1), for FW and BW operations is shown in Fig. 8.a. In the region $\beta < 0.28$ BW operation provides the higher value of accelerating gradient. Due to longer cells d_p , (2), and higher Q values (see Fig. 3), DLW in BW mode has all time smaller attenuation constant α , Fig. 7,b. The plots of optimal $\theta(\beta)$ values to get the maximal E_n are shown in Fig. 7,c.

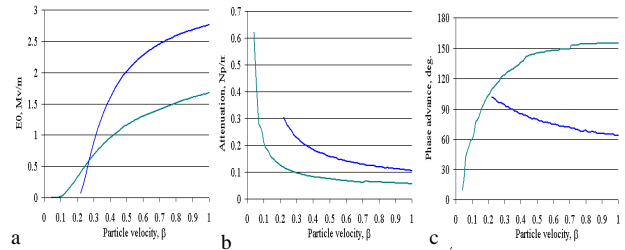


Fig. 7. The plots of the maximal E_0 values assuming $P_t=1$ MW, $\beta_g=0.01$ (a), corresponding plots of attenuation α (b), and optimal phase advance θ (c). The blue curves correspond to FW $n=0$ operation, the green curves are for BW $n=-1$ operation, $t=5$ mm

As one can see from Fig. 7,a, both for BW and FW operation the maximal E_n value increases with β increasing. For BW operation $\beta_g < 0$ and RF input is places in the higher β section end, where the higher E_{-1} value can be achieved and attenuation α is lower. It leads to the higher δW for BW DLW section, as compared to FW DLW, in the wider region of particles velocity, $\beta < (0.4 \sim 0.5)$.

To extend accelerating DLW structure to low β region, the BW operating mode is more effective.

3. DESIGN APPROACH AND EXAMPLES OF DLW ACCELERATING SYSTEM

The main guideline for design of DLW sections is the maximal possible accelerating gradient, leading to the maximal δW both for each DLW section, but with considerations of reasonable practical possibilities.

The design approach, RF power requirements and safety margins for accelerating system design is considered in [7] with more details.

The main parameter for the choice is the β_g values in the sections. To overlap the wide β region, DLW system should use BW operating mode for the low β and usual FW operation mode for the moderate and the high β parts. Taking into account reasons of practical realizations and sections tuning, at first we suggest the same minimal β_g value in all DLW sections in the system, both for BW and for FW parts. The option of $\beta_g = \text{const}$ in BW allows much higher E_{\perp} values and corresponding δW gain for the same length. A growing along section E_{\perp} is realized, providing some advantages in particle dynamics. For FW sections the constant gradient option is realized. The RF sources suggest the modern klystrons with RF pulse compression technique.

Because the value $\beta_{gou} = 0.4\%$ is the minimal value, which was realized in L-band practice, [1], it was considered first and start with $\beta > 0.08$. Due to start with very low β value and short cell length d_p , in the first BW section the iris thickness is $t=3.5$ mm and $t=5$ mm for another. The option results in 8 sections with the total length $L_t = 22.72$ m, the total traversing time $T_f = 126$ ns and $\Delta W = 218.7$ MeV, exceeding the required value $\Delta W \sim 195$ MeV. But, as shows more detailed analysis, the initial part of the first BW section, near 50 cells, accelerate with very low efficiency, due to low E_{\perp} value (see Fig. 7,a). The DLW beginning from $\beta > 0.2$ leads to much better results of entire accelerating system, [7], both in $\Delta W = 229.7$ MeV and in the traversing time for muons, $T_f \sim 108$ ns. The extra ΔW can be spend for β_{gou} increasing to 0.6%. The further operation β_{gou} increasing leads to the increasing of the system length and looks not attractive. Without essential deterioration of the total system parameters β_{gou} can be increased for BW sections, realizing the higher β_{gou} in BW part and the lower – in FW part. The examples of DLW accelerating systems are described in details in [7] and the short summary is in the Table.

The summary for examples of accelerating systems with DLW sections

	1	2	3	4	5	6
$P_{\text{tot}} = \Sigma P_t$, MW	144	144	144	144	144	216
$\beta_{gou} \%$	0.4	0.4	0.6	0.75	0.75-0.6	0.9-0.8
β_{in}	0.08	0.2	0.2	0.2	0.2	0.2
$\Delta W = \Sigma \delta W$, MeV	218,7	229.7	195.6	195.7	195.6	193.2
$L_t = \Sigma L$, m	22.72	22,79	22.75	25.66	23.52	18.88
$N_t = \Sigma N$	362	352	370	420	385	303
$T_c^t = \Sigma T_c$, 10^3	78.5	65.7	50.2	46.7	45.8	36.9
$T_f = \Sigma t_f$, ns	126	108	113	130	120	98

3.1. RESULTS CONSIDERATION

As it should be for the L-band frequency, possible options can be obtained at the expense of high input RF power and not so high group velocity. But, starting from example in [7], we consider β_{gou} for accelerating sections, which is not less than the maximal β_{gin} value in already realized references, [1]. As one can see from the summarizing Table, required number of DLW sections is not so big. At least, with 8 sections the goal $\Delta W \sim 195$ MeV can be achieved, assuming $\beta_g > 0.6\%$. It is not so small group velocity, even for the S-band range. It may be mentioned here, that in the classical S-band constant gradient accelerating sections, with 10 foot length, in the Stanford two-mile accelerator the group velocity changes as $2.04\% > \beta_g > 0.65\%$.

Also consideration shows variety of different possibilities. In the practical linac design all parameters should be balanced. The results, presented in the Table 1 show some limitations and some trends of results change in dependence on input data.

Results of the study show some practical benefits for FW DLW sections realization with $\theta \sim 120^\circ$. With a quite small loss $< 3\%$ in the energy gain one can obtain quite visible reduction of efforts in the tuning of accelerating sections. Another attractive feature is larger cell length, which, together with the reduced thickness of the iris, provides comfortable spacing between adjacent irises for low β range.

4. SOME REMARKS FOR BEAM DYNAMICS

The particles dynamics is not considered in this work, just very approximately a longitudinal bunch length and longitudinal oscillations are taken in consideration by the synchronous phase $\phi_s \sim 30 \dots 10^\circ$ assuming the bunch length reduction with energy increasing. Acceleration of muons with a relative high frequency DLW structure is possible (or practically reasonable) from low energy $W_m \sim 107.84$ MeV. Below this energy enough narrow range ~ 3 MeV should be covered with another structures, with lower operating frequency. The matching technique in longitudinal motion is known in high energy proton linacs.

More interesting is one possibility for particles focusing in BW DLW sections. There are well known two methods of focusing with RF fields – Radio Frequency Quadrupole (RFQ) and Alternating Phase Focusing (APF). There is a third idea of particle focusing by the fast not synchronous spatial harmonic. In BW DLW the synchronous harmonic $n = -1$, is not fundamental and all time exists harmonic $n = 0$ with larger amplitude and higher phase velocity. As it was shown in [10], such fast harmonic can provide the focusing effect. This effect was investigated theoretically for focusing in proton accelerators, see [11] with appropriate references. In the practical realization for electron linac, [4, 5], the pulse current up to 2 A was obtained in the BW DLW section, $\theta = 120^\circ$, without external magnetic focusing.

For muons acceleration this backward mode is suggested to extend the same structure - DLW - to middle and low β range and we have already the fast harmonic in BW sections. The beam intensity for muons is negli-

gible and requirements for the transverse motion stability looks more relaxed, as compared to [11], [4].

It is attractive to estimate such possibility for BW DLW sections. If the focusing effect will be sufficient, the particles focusing in the BW DLW section will be free of any additional charge, just as the sequence of DLW application.

SUMMARY

The well known DLW accelerating structure is considered in details for applications in the L-band frequency range and for accelerating of particles with intermediate mass in the wide range of particles velocity.

For the L-band range the dimensions of cells can be optimized in the iris thickness to have higher accelerating gradient, lower attenuation and larger space between irises. By choosing phase advance $\theta=120^\circ$, we can propose DLW accelerating system, which overlap simultaneously both high particle energy range and moderate energy range too with essentially reduced number of cells. With application of the backward wave operating mode we can extend DLW structure to low β . Combining BW operating mode in the system beginning and FW operating mode for medium and high particles energy, we can suggest DLW accelerating system, which overlap the muons velocity range from $\beta \sim 0.2$ to $\beta \sim 0.93$ with 8 or 6 accelerating sections, just using two or three RF sources with RF pulse compression.

As compared to another possible solutions for low and medium energy range, such accelerating system has the preferences of uniformity, simplicity and cost efficiency.

REFERENCES

1. S. Matsumoto et al. L-band accelerator system in injector linac for SuperKEKB // *Proc. of the IPAC 2010, Kyoto, Japan*. 2010, p. 3708.
2. J.W. Wang et al. Studies of room temperature structures for the ILC positron source // *Proc. of the 2005 PAC*. 2005, p. 2827.

3. G. Loew, R. Neal. Accelerating Structures, G. Dome. Review and Survey of Accelerating Structures // *Linear Accelerators* / Ed. P. Lapostolle, E. Septier, Amsterdam, 1970.
4. M.I. Aizatsky et al. High current electron linac for investigations in new methods of acceleration // *Fizika plazmy*. 1994, v. 20, №7, 8, p. 671 (in Russian).
5. A.N. Dovbnya et al. Beam parameters of an S-band electron linac with beam energy of 30...100 MeV // *Problems of Atomic Science and Technology. Series «Nuclear Physics Investigations»*. 2006, v. 46, №2, p. 11-13.
6. V. Paramonov. The data library for accelerating structures development // *Proc. of the 1996 LINAC Conference*, Geneva, CERN. 1996, v. 2, p. 493.
7. V. Paramonov. Parameters of the Disk Loaded Waveguide structure for intermediate particles acceleration in the intermediate energy range. *arXiv:1307.6506v1, [physics.acc.ph]*, July 2013.
8. T. Khabiboulline, V. Puntus, et al. A new tuning method for traveling wave structures // *Proc. of the 1995 PAC*, p. 1666.
9. S. Artikova, F. Naito, M. Yoshida. The accelerator design of muon g-2 experiment at J-PARC // *Proc. Of the 2013 IPAC*, p.1334. Conceptual design report for the measurement of the muon anomalous magnetic moment g-2 and electric dipole moment at J-PARC, December 13, 2011.
10. V. Tkalich // *Zh. Eksp. Teor. Fiz.* 1957, v. 32, p. 625; *Sov. Phys. JETP*. 1957, v. 5.
11. V. Baev, S. Minaev. Efficiency of ion focusing by the field of a traveling wave in a linear accelerator // *Zh. Tekh. Fiz.* 1981, v. 51, p. 2310; *Sov. Phys. Tech. Phys.* 1981, v. 26(11).

Article received 08.09.2013

ХАРАКТЕРИСТИКИ КРУГЛОГО ДИАФРАГМИРОВАННОГО ВОЛНОВОДА ДЛЯ УСКОРЕНИЯ ЧАСТИЦ ПРОМЕЖУТОЧНОЙ МАССЫ В ДИАПАЗОНЕ СРЕДНИХ ЭНЕРГИЙ

В.В. Парамонов

Рассчитаны параметры круглого диафрагмированного волновода (КДВ) на рабочей частоте L-диапазона для прямой и обратной волн в диапазоне скорости синхронной частицы $0,04 < \beta < 1$. Показано, что при использовании особенностей ускорения бегущей волной, оптимизации размеров ячеек КДВ, выборе оптимального вида колебания для каждой секции и сочетания режимов обратной и прямой волн можно создать в диапазоне скоростей мезонов $0,2 < \beta < 1$ ускоряющую систему на основе КДВ, превосходящую по параметрам качества возможные варианты с резонаторами на стоячей волне.

ХАРАКТЕРИСТИКИ КРУГЛОГО ДИАФРАГМОВАНОГО ХВИЛЕВОДА ДЛЯ ПРИСКОРЕННЯ ЧАСТИНОК ПРОМІЖНОЇ МАСИ У ДІАПАЗОНІ СЕРЕДНІХ ЕНЕРГІЙ

В.В. Парамонов

Розраховано параметри круглого діафрагмованого хвилеводу (КДХ) на робочій частоті L-діапазону для прямої і зворотної хвилі у діапазоні швидкості синхронної частинки $0,04 < \beta < 1$. Показано, що при використанні особливостей прискорення хвилею, що біжить, оптимізації розмірів осередків КДХ, виборі оптимального виду коливання для кожної секції і поєднання режимів зворотної та прямої хвилі можна створити в діапазоні швидкостей мезонів $0,2 < \beta < 1$ прискорюючу систему на основі КДХ, що перевершує за параметрами якості можливі варіанти з резонаторами на стоячій хвилі.